

Methyl Formate Production on TiO₂(110), Initiated by Methanol Photocatalysis at 400 nm

Qing Guo,^{†,⊥} Chenbiao Xu,^{†,||,⊥} Wenshao Yang,[†] Zefeng Ren,[§] Zhibo Ma,[†] Dongxu Dai,[†] Timothy K. Minton,^{*,‡,¶} and Xueming Yang^{*,†}

[†]State Key Laboratory of Molecular Reaction Dynamics, Dalian Institute of Chemical Physics, 457 Zhongshan Road, Dalian 116023, Liaoning, P. R. China

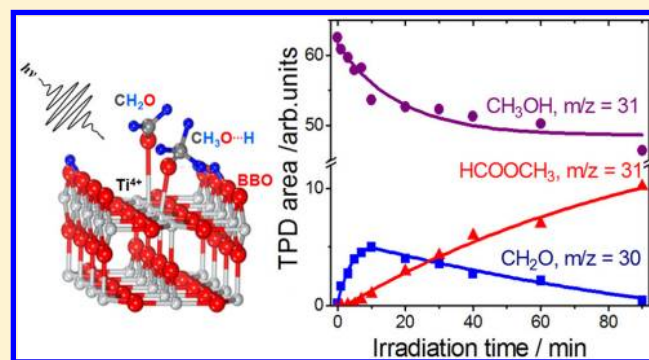
[‡]Department of Chemistry and Biochemistry, Montana State University, Bozeman, Montana 59717, United States

[§]International Center for Quantum Materials, Peking University, Beijing 100871, P. R. China

^{||}School of Physics and Optoelectric Engineering, Dalian University of Technology, Dalian, Liaoning 116023, P. R. China

S Supporting Information

ABSTRACT: Previous observations of methyl formate (HCOOCH₃) during the photo-oxidation of methanol (CH₃OH) on TiO₂ catalysts suggested that photocatalysis on TiO₂ could be used to build up complex molecules from a single precursor. We have investigated the mechanism of HCOOCH₃ formation by irradiating a CH₃OH-adsorbed TiO₂(110) surface with 400 nm light at low surface temperatures. Through the detection of volatile products after irradiation by temperature programmed desorption, we have found, as previously reported [Phillips et al. *J. Am. Chem. Soc.* **2013**, *135*, 574–577] that HCOOCH₃ is formed by the cross-coupling reaction of CH₃O and CH₂O, which are products of the first and second dissociation steps, respectively, in the stepwise photocatalysis of CH₃OH on TiO₂(110). Unlike the previous study, we have observed the photocatalytic production of HCOOCH₃ without preoxidation of the surface, and we have concluded that the final reaction step to produce HCOOCH₃ (i.e., the cross-coupling reaction of CH₂O with CH₃O) does not involve a transient HCO intermediate.



I. INTRODUCTION

The potential value of TiO₂ in biomass conversion into fuels and useful synthetic chemicals^{1–7} has inspired enormous interest in replacing current technology for stoichiometric oxidation of alcohols⁸ with photocatalytic processes on TiO₂ that could reduce energy consumption, minimize environmental pollutants, and increase selectivity.^{9–13} Although CH₃OH is often used in benchmark studies of the photocatalytic properties of TiO₂,^{2,7,14–21} there have been only a few studies on selective oxidation of CH₃OH over TiO₂ photocatalysts.^{3,4,14,15,19,22} Various products were observed, such as H₂, CO, CO₂, CH₂O, HCOOH, and HCOOCH₃, but the mechanisms of methanol photo-oxidation remain unclear. The presence of HCOOCH₃ (methyl formate) suggests that synthetic reactions, catalyzed on surfaces by light, could be used to build complex molecules from a single precursor. In a recent study employing temperature programmed desorption (TPD) and scanning tunneling microscopy (STM), Friend and co-workers have deduced the mechanism of CH₃OH photo-oxidation on a preoxidized TiO₂(110) surface.²³ They concluded that coadsorbed oxygen atoms first reacted thermally with CH₃OH to produce adsorbed CH₃O and H₂O. Then CH₃O underwent photo-oxidation to HCOOCH₃ in a two-step

process where the CH₃O dissociated to CH₂O and a cross-coupling reaction involving an HCO intermediate led to the formation of HCOOCH₃. In this study, the preoxidation of the surface was considered to be essential to the initial formation of adsorbed CH₃O, and the HCO intermediate was an indication of the hole-mediated dissociation of CH₂O by a bridge-bonded oxygen (BBO) atom.

Our earlier TPD study of CD₃OH photo-oxidation on TiO₂(110) described the stepwise dissociation to CD₃O and CD₂O in the absence of coadsorbed oxygen.²⁴ We have extended these experiments and have observed methyl formate production with a significant isotope effect. The photocatalytic transformation of CH₃OH into HCOOCH₃ on TiO₂(110) proceeds rapidly, while that of CD₃OH is negligible on the time scales studied. The use of isotopic substitution to stop the photo-oxidation process before the final coupling step to produce methyl formate has allowed us to demonstrate that the formyl species (HCO/DCO) is not an intermediate in this step, thus calling into question the hole-mediated dissociation mechanism of formaldehyde.

Received: February 14, 2013

Published: February 22, 2013

Clean $\text{TiO}_2(110)$ surfaces were dosed, typically at 120 K, with various coverages of precursor molecules before irradiation with 400 nm light, and products were detected by TPD subsequent to irradiation or by a time-of-flight (TOF) method during irradiation. Several experiments were performed in order to verify the cross-coupling mechanism starting from a single CH_3OH precursor on a pristine $\text{TiO}_2(110)$ surface and to probe the possible formyl intermediate in the cross-coupling step.

II. EXPERIMENTAL DETAILS

The TPD apparatus has been described previously.²⁴ The base pressure of the sample chamber is $<6 \times 10^{-11}$ Torr. A quadrupole mass spectrometer (Extrel) is used to detect desorbed products. An extremely high vacuum of 1.5×10^{-12} Torr in the electron-impact ionization region was achieved and maintained during the experiment. The $\text{TiO}_2(110)$ (Princeton Scientific) sample had dimensions of 10 mm \times 10 mm \times 1 mm. The surface was cleaned by cycles of Ar^+ sputtering and resistive heating to 850 K in vacuum; 1000 eV Ar^+ was used for the initial cycles until impurities of Ca, Na, K, and C were no longer observed by Auger electron spectroscopy. For subsequent cycles, 500 eV Ar^+ was used to flatten the surface. The $\text{TiO}_2(110)$ surface contained 3–4% O-vacancy defects as determined by H_2O TPD.²⁵ CH_3OH (Aldrich, 99.9+ %) was further purified by several freeze–pump–thaw cycles before use and introduced into the sample chamber with a calibrated molecular beam doser. The surface temperature was maintained at 120 K during CH_3OH dosing, and it typically rose to ~ 180 K during subsequent irradiation. The irradiating light came from a frequency doubled Ti:Sapphire femtosecond laser at 400 nm (Coherent, repetition rate 1 kHz). Unless otherwise stated, the average intensity of the laser beam on the sample was 400 mW with a diameter of 6 mm, corresponding to about 1.44×10^{18} photons $\text{cm}^{-2} \text{s}^{-1}$. The light was incident on the $\text{TiO}_2(110)$ at $\sim 30^\circ$ with respect to $\text{TiO}_2(110)$ surface. TPD signals were collected after irradiation with a heating rate of 2 K/s and with the sample facing the mass spectrometer detector. To exclude effects from nonlinearity that might result from the relatively high photon fluxes used, we studied the power dependence of the primary CH_2O and secondary HCOOCH_3 products that were detected in our experiments (see Figure S1 of Supporting Information). We have observed no evidence that the photon fluxes used in our experiments would impart any anomalous behavior in our results arising from multiphoton effects.

III. RESULTS AND ANALYSIS

Figure 1 shows TPD spectra collected at the CH_2O parent mass-to-charge ratio, $m/z = 30$, corresponding to various irradiation times. Dissociative ionization of CH_3OH in the electron-impact ionizer may lead to a signal at $m/z = 30$, as evidenced by the TPD peak near 290 K when no UV irradiation is used.¹⁰ Note that the CH_3OH desorption TPD spectrum does not show a peak at 640 K unless the surface is predosed with O_2 .^{10,23,26} After 400 nm irradiation, a peak appears at 260 K in the TPD spectrum and first increases and then decreases in magnitude with increasing irradiation time. This peak is assigned to CH_2O based on earlier studies from our lab²⁴ and others.^{25,27} The near disappearance of this peak after an irradiation time of 90 min might be explained by photoinduced desorption or chemical conversion of CH_2O .

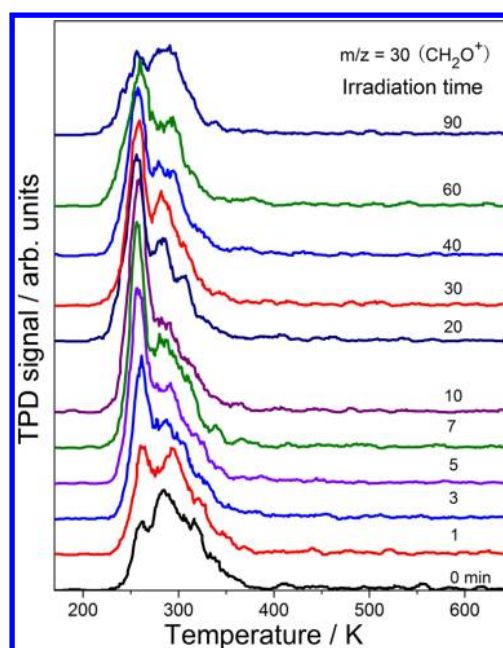


Figure 1. TPD spectra acquired at $m/z = 30$ after 0.5 ML of CH_3OH was adsorbed on $\text{TiO}_2(110)$ at 120 K and irradiated at 400 nm for various times, as indicated.

To determine whether conversion to HCOOCH_3 was the reason for the disappearance of CH_2O , we collected TPD spectra at $m/z = 31$ (CH_3O^+) for various irradiation times (see Figure 2). This m/z ratio was selected because it conveys a

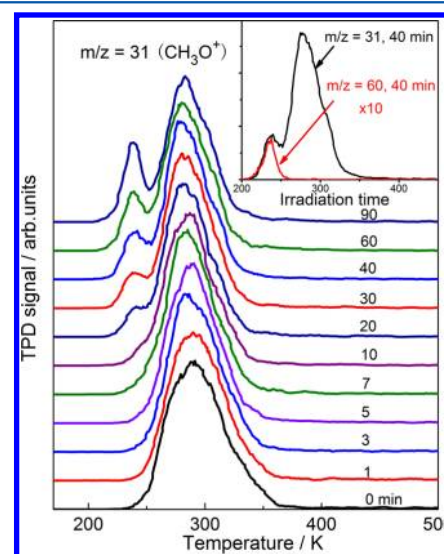


Figure 2. TPD spectra acquired at $m/z = 31$ after 0.5 ML of CH_3OH was adsorbed on $\text{TiO}_2(110)$ at 120 K and irradiated at 400 nm for various times, as indicated. Inset shows a comparison between TPD spectra acquired at $m/z = 31$ and 60 after 40 min of irradiation time. We typically observe no CH_3OH TPD peak at 350 K with the Ar^+ sputtering conditions used in our experiments.

signal from all CH_3O -containing species that may dissociatively ionize, such as CH_3OH and HCOOCH_3 . The main TPD peak, centered at 290 K, comes from CH_3OH . As the irradiation time increases, the CH_3OH TPD peak decreases in intensity and shifts toward lower temperatures, which was discussed in our earlier paper.²⁴ At longer irradiation times, a second peak

appears as a shoulder at low temperatures, near 235 K, and increases in magnitude with increasing irradiation time. This low-temperature shoulder has the same TPD temperature and shape as the only peak observed in the $m/z = 60$ TPD spectrum (see inset in Figure 2), which corresponds to the parent m/z ratio of HCOOCH_3^+ . However, according to ESD work involving CH_3OH on $\text{Ag}(111)$ by Schwane and White,²⁸ the $m/z = 60$ peak could arise from HOCH_2CHO (glycolaldehyde) or HCOOCH_3 .

Additional TPD traces help to distinguish between the two possible products detected at $m/z = 60$. TPD traces for $m/z = 15(\text{CH}_3^+)$, $18(\text{H}_2\text{O}^+)$, $28(\text{CO}^+)$, $29(\text{CHO}^+)$, $30(\text{CH}_2\text{O}^+)$, and $32(\text{CH}_3\text{OH}^+)$ were measured following an irradiation time of 30 min (see Figure S2, Supporting Information). All TPD spectra show the appearance of an additional peak near 235 K after irradiation, except for the spectrum collected at $m/z = 18$. The lack of an additional $m/z = 18$ peak following laser irradiation leads to the conclusion that the product that desorbs at 235 K is HCOOCH_3 and not HOCH_2CHO .²⁹

Figure 3 shows a comparison of the rates of destruction of CH_3OH and formation of CH_2O and HCOOCH_3 by showing

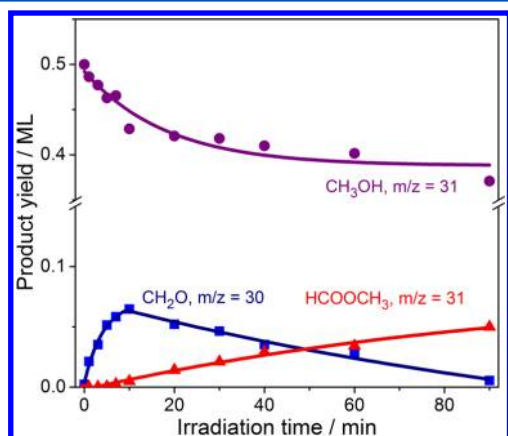


Figure 3. Yields of CH_3OH , CH_2O , and HCOOCH_3 as a function of irradiation time, derived from data in Figures 1 and 2.

the yields of these species as a function of irradiation time for 0.5 ML of CH_3OH adsorbed initially on $\text{TiO}_2(110)$. Figure S3, Supporting Information, shows the yields for the analogous deuterated species when 0.5 ML of CD_3OH is adsorbed initially on $\text{TiO}_2(110)$, where the DCOOCd_3 yield has been included with the already published yields of CD_3OH and CD_2O .²⁴ As can be seen in Figure 3, during the first 10 min of irradiation, the amount of CH_2O produced rises rapidly to a maximum, while hardly any HCOOCH_3 is formed. Longer irradiation times lead to a steady decrease in the amount of CH_2O and a concomitant increase in the amount of HCOOCH_3 . After 90 min of irradiation, very little CH_2O remains. Thus, the formation of HCOOCH_3 appears to be directly correlated with the depletion of CH_2O . The rate of methyl formate formation exhibits a significant isotope effect. As shown in Figure S3, Supporting Information, when CD_3OH is used as the precursor, the yield of DCOOCd_3 is negligible on the time scales used in our experiments.

To confirm that the formation of HCOOCH_3 proceeds through coupling reactions involving CH_2O , we studied the dependence of the HCOOCH_3 TPD signal on the initial coverage of CH_3OH (see Figure 4, which shows a summary of the data presented in Figure S4, Supporting Information). After

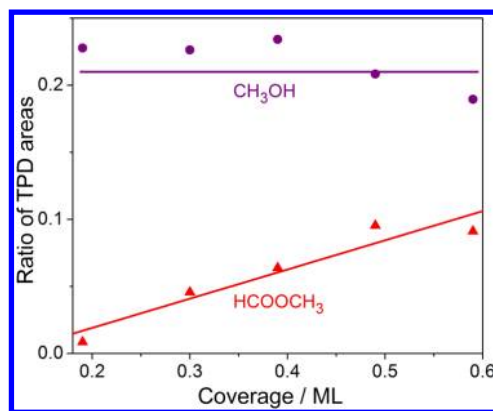


Figure 4. CH_3OH and HCOOCH_3 signals acquired at $m/z = 31$ as a function of initial CH_3OH coverage on a $\text{TiO}_2(110)$ surface, with 30 min of 400 nm irradiation. At each coverage, the CH_3OH and HCOOCH_3 signals shown are ratios of the integrated TPD signals for the respective species to the integrated TPD signal of CH_3OH acquired at $m/z = 31$ without irradiation.

30 min of irradiation time, the TPD yield for CH_3OH decreases by roughly 20–22% regardless of its initial coverage, whereas the HCOOCH_3 signal, normalized to the initial coverage of CH_3OH , increases roughly linearly with the initial coverage of CH_3OH . On the basis of previous studies, the saturated first layer adsorption of CH_3OH on $\text{TiO}_2(110)$ varies between 0.67 and 0.77 ML,^{10,30} which implies that there are two adsorbed CH_3OH molecules per three Ti^{4+} sites or three adsorbed CH_3OH molecules per four Ti^{4+} sites when the first layer of adsorption is saturated. With increasing CH_3OH coverage, the HCOOCH_3 yield increases together with the probability of two CH_3OH molecules being adsorbed nearby each other. Thus, the clear dependence of HCOOCH_3 yield on CH_3OH coverage, combined with the anticorrelation between CH_2O and HCOOCH_3 product yields at long irradiation times (see Figure 3), strongly suggests that HCOOCH_3 formation is the result of coupling reactions between CH_2O and another reactive species that is connected with the initial presence of CH_3OH . Irradiation of the surface by 400 nm light produces CH_2O , which is evidently involved in the production of HCOOCH_3 .

A series of thermal catalytic investigations on gas-phase dehydrogenation of CH_3OH to HCOOCH_3 over copper-based catalysts^{31–34} concluded that the formation of HCOOCH_3 in the absence of O_2 occurs either through a hemiacetal (reaction of CH_3OH or CH_3O with CH_2O) or a Tishchenko (reaction of two CH_2O molecules) mechanism. The recent work of Friend and co-workers on the photo-oxidation of CH_3OH on a preoxidized $\text{Ti}(110)$ surface suggests that HCOOCH_3 is formed exclusively through the cross-coupling reaction of CH_3O and CH_2O intermediates.²³ Both CH_3O and CH_2O are also available under our experimental conditions, as we have recently shown that CH_2O is formed through the stepwise photocatalysis of CH_3OH on $\text{TiO}_2(110)$, with CH_3O as the intermediate species. Indeed, through an experiment involving surfaces on which CH_3OH and CD_3OH were coadsorbed, we found that the cross-coupling reaction occurs (see Figure 5), and in a separate experiment that started with adsorbed CH_2O , we saw no evidence for formation of HCOOCH_3 , indicating that the self-coupling reaction does not occur (Figure 6). Thus, we conclude that the cross-coupling reaction also proceeds

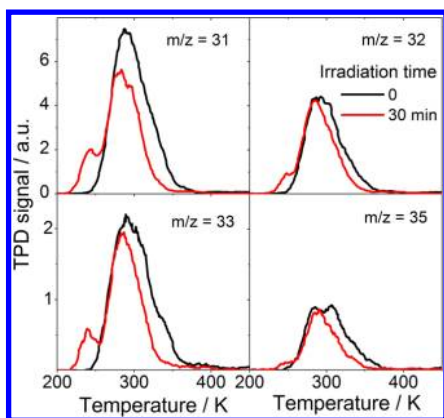


Figure 5. TPD spectra acquired at $m/z = 31$ (CH_3O^+ , CHDO^+), 32 (CH_4O^+ , CH_2DO^+ , CD_2O^+), 33 (CHD_2O^+ , CH_3DO^+), and 35 (CHD_3O^+) after 0.35 ML of CH_3OH and 0.15 ML of CD_3OH were coadsorbed on $\text{TiO}_2(110)$ at 105 K and irradiated at 400 nm for 0 (black) and 30 min (red). CD_3OH was dosed first. The m/z ratios correspond to fragments of various possible isotopic variants of methanol, formaldehyde, and methyl formate. In all these spectra, the large peaks at ~ 290 K arise from desorption of methanol, and the shoulders at lower temperatures may come from either formaldehyde or methyl formate. The shoulder in the TPD spectrum collected at $m/z = 35$ could only come from a fragment of HCOOCD_3 , formed from a cross-coupling reaction of CH_2O and CD_3O . Thus, the cross-coupling reaction clearly occurs.

exclusively under our experimental conditions, with irradiation at 400 nm.

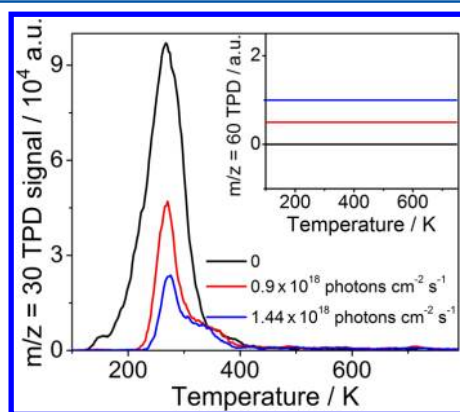


Figure 6. TPD spectra acquired at $m/z = 30$ (CH_2O^+) after 0.55 ML of CH_2O was dosed on $\text{TiO}_2(110)$ and either not irradiated or irradiated with different photon fluxes, as shown, for 30 min. The inset shows that no TPD signal was observed at $m/z = 60$ (HCOOCH_3^+) under any of these conditions. The lack of HCOOCH_3 indicates that the self-coupling reaction of CH_2O does not occur.

An experiment with coadsorbed CH_3O and CH_2O was performed to verify that the cross-coupling reaction was photocatalyzed and occurred during irradiation, rather than during TPD via a thermal mechanism. As shown in Figure 7, with 0.14 ML of CH_3O and 0.5 ML of CH_2O initially coadsorbed on the $\text{TiO}_2(110)$ surface, no HCOOCH_3 signal could be observed during TPD of the unirradiated surface. Thus, heating does not promote the reaction on a $\text{TiO}_2(110)$ surface. Note that the coupling of CH_3O and CH_2O does, however, occur thermally on a $\text{Au}(111)$ surface.^{35–39}

H atoms were also detected (via TPD of H_2O) from irradiation of CH_3OH -adsorbed $\text{TiO}_2(110)$, and their coverage

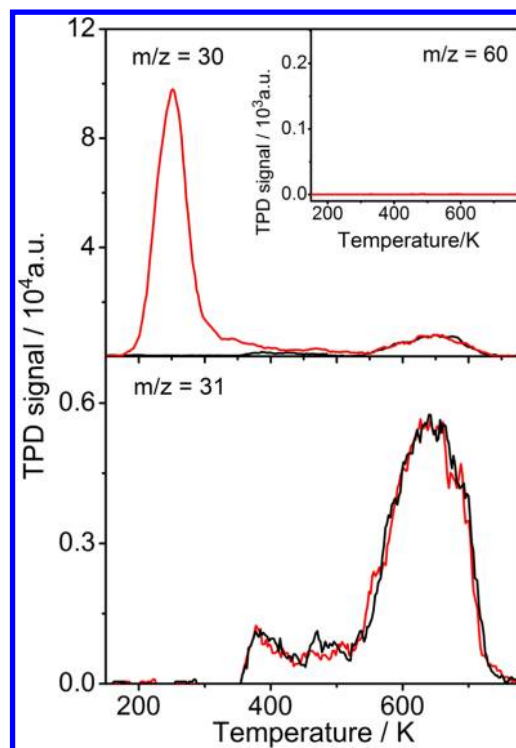


Figure 7. TPD spectra acquired at $m/z = 30$ (CH_2O^+), $m/z = 31$ (CH_3O^+), and $m/z = 60$ (CH_4O_2^+) from 0.14 ML of CH_3O adsorbed on $\text{TiO}_2(110)$ (black line) and 0.14 ML of CH_3O and 0.5 ML of CH_2O coadsorbed on $\text{TiO}_2(110)$ (red line). Surface methoxy groups were produced by sequential dosing of oxygen and methanol gases, followed by flashing the sample to 350 K to remove water and molecularly adsorbed methanol.^{10,26} As shown in the inset, no signal at $m/z = 60$ (HCOOCH_3^+) was observed with CH_2O and CH_3O coadsorbed on a $\text{TiO}_2(110)$ surface, implying that the cross coupling reaction to produce HCOOCH_3 was photocatalyzed and did not occur thermally during TPD. The 640 K peak in both TPD spectra arises from CH_3O disproportionation, as has been discussed previously.²⁶

corresponds mainly to H atoms produced by dissociation of CH_3OH as it underwent the loss of two H atoms to form CH_2O . Before irradiation, the H-atom coverage was about 0.03 ML. After 90 min of irradiation, 0.24 ML of H atoms on BBO sites remained (Figure 8), consistent with the 0.13 ML of CH_3OH depletion observed in Figure 3. A tiny amount of H_2 might have been produced from recombination, but these signals were below our detection limit.

As depicted in Figure 6, no HCOOCH_3 was observed after irradiation of the $\text{TiO}_2(110)$ surface with adsorbed CH_2O , even though a large fraction of the CH_2O coverage disappears during 30 min of irradiation. A small fraction of the CH_2O product desorbs during irradiation, as evidenced by a TOF signal of CH_2O (Figure 9), which corresponds to desorption of ~ 0.01 ML during the first 30 min of irradiation. Most of the disappearance of CH_2O appears to be from conversion to formate, as revealed in the TPD spectra shown in Figure 10, which were collected at $m/z = 28$ (C_2H_4^+ , CO^+), 29 (CHO^+), 30 (CH_2O^+), 44 (CO_2^+), 45 (HCOO^+), and 46 (HCOOH^+). Two new desorption features at 486 and 587 K appear in the $m/z = 29$ TPD spectrum with 30 min of irradiation, suggesting that the new features are possibly the result of photocatalytic products. Using previous studies of HCOOH adsorbed on $\text{TiO}_2(110)$ ⁴⁰ and the cracking pattern of HCOOH collected with our mass spectrometer, we concluded that the 486 K peak

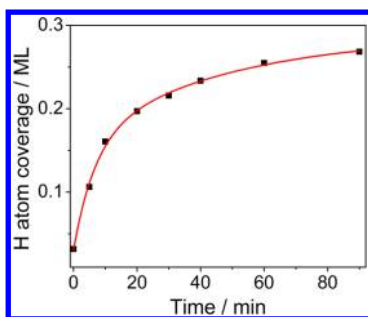


Figure 8. H-atom coverage on BBO sites as a function of irradiation time at 400 nm (laser flux = 1.44×10^{18} photons $\text{cm}^{-2} \text{s}^{-1}$) for 0.5 ML of CH_3OH adsorbed initially on $\text{TiO}_2(110)$. The decomposition of CH_3OH to CH_2O and HCOOCH_3 results in surplus H atoms, which transfer to BBO sites. During TPD, the H atoms combine with BBO atoms to produce desorbed H_2O . On the basis of the peak area of the first layer water desorption, the H-atom coverage on BBO sites can be determined from the measured peak area. It is clear from these data that the depletion of CH_3OH is the result of H-atom dissociation.

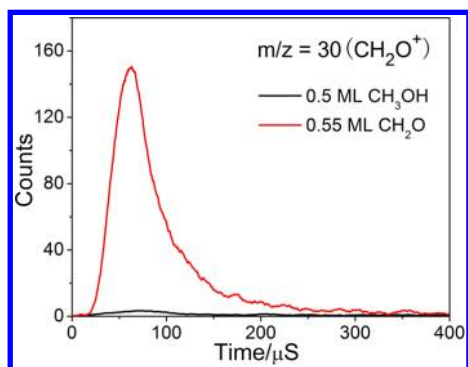


Figure 9. TOF signals of CH_2O , ejected from 0.55 ML^{10,30} of CH_2O -adsorbed $\text{TiO}_2(110)$ (black line) and from 0.5 ML CH_3OH -adsorbed $\text{TiO}_2(110)$ during irradiation (red line). On the basis of quantitative coverages derived from the data shown in Figure 6, after 400 nm of irradiation for 30 min (with a laser flux of 1.44×10^{18} photons $\text{cm}^{-2} \text{s}^{-1}$), 0.08 ML of CH_2O was left on the surface, and about 0.15 ML of CH_2O transferred to other products, such as HCOOH , CH_3 , and formates. From the areas of the TOF signals, we conclude that about 0.01 ML of CH_2O was desorbed during the first 30 min of irradiation of a $\text{TiO}_2(110)$ surface with 0.5 ML of CH_3OH adsorbed.

at $m/z = 29, 44, 45$, and 46 is desorbed HCOOH , which results from the recombination of surface formates with surface hydroxyl groups. The 587 K peak at $m/z = 28, 29$, and 44 is assigned to desorption of surface formates in the form of CO , HCO , and CO_2 . Previous investigations on the photochemistry of acetone and acetaldehyde on preoxidized $\text{TiO}_2(110)$ ^{41–47} show that acetone or acetaldehyde adsorbed on oxidized $\text{TiO}_2(110)$ undergoes a facile thermal reaction to form a photoactive acetone–oxygen or acetaldehyde–oxygen complex first, and then ultraviolet (UV) light irradiation of the acetone–oxygen or acetaldehyde–oxygen complex results in the ejection of methyl radical into gas phase and conversion of the surface bound fragment to acetate or formate. Here, without a preoxidized $\text{TiO}_2(110)$ surface, the main product, formate, was still observed in our experiments, implying that a photoactive $\text{H}_2\text{CO}-\text{O}$ complex was formed during UV irradiation and suggesting that bridge-bonded O atoms are involved in the complex. Taking into account mass spectrometer sensitivity factors, the yield of CO is about 0.08 ML after 30 min of irradiation.

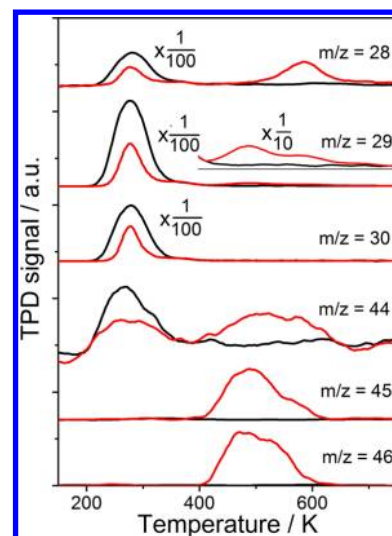


Figure 10. TPD spectra acquired at $m/z = 28(\text{C}_2\text{H}_4^+, \text{CO}^+)$, $29(\text{CHO}^+)$, $30(\text{CH}_2\text{O}^+)$, $44(\text{CO}_2^+)$, $45(\text{HCOO}^+)$, and $46(\text{HCOOH}^+)$ after 0.55 ML of CH_2O was adsorbed on $\text{TiO}_2(110)$ at 110 K and irradiated for 0 (black) and 30 min (red) with 400 nm light at 0.54×10^{18} photons $\text{cm}^{-2} \text{s}^{-1}$. The 486 K peak at $m/z = 29, 44, 45$, and 46 is desorbed HCOOH , which results from the recombination of surface formates with surface hydroxyl groups. The 587 K peak at $m/z = 28, 29$, and 44 is assigned to desorption of surface formates in the form of CO , HCO , and CO_2 .

IV. DISCUSSION

Previous studies from our group²⁴ and others^{48–50} indicate that the molecular state of methanol adsorbed on a Ti^{4+} site is nearly isoenergetic with the dissociated state ($\text{CH}_3\text{O} + \text{H}$) and that the barrier between these states is very low. Hence, the two states should coexist in equilibrium even at low surface temperatures. In order for the cross-coupling reaction to be promoted by heat, the CH_3O intermediate species would have to persist after irradiation. However, the easy back reaction, $\text{CH}_3\text{O} + \text{H} \rightarrow \text{CH}_3\text{OH}$, should remove CH_3O in the form of CH_3OH during TPD. Furthermore, the relatively easy forward reaction, $\text{CH}_3\text{O} \rightarrow \text{CH}_2\text{O} + \text{H}$ with UV radiation would make it very unlikely that CH_3O is available for cross-coupling reactions, especially after long irradiation times.^{23–25} The facts that (1) CH_3O must be efficiently removed by back-reacting to CH_3OH during TPD and that (2) the yield of HCOOCH_3 increases with irradiation time are consistent with the conclusion that the cross-coupling reaction of CH_3O and CH_2O in our experiment occurs during irradiation and not when the surface is heated for the TPD measurement.

Recent thermal catalytic studies are consistent with a preference of cross-coupling over self-coupling. A study of CH_2O polymerization on $(\text{WO}_3)_3/\text{TiO}_2(110)$ shows that no $(\text{CH}_2\text{O})_n$ desorption was observed on a bare $\text{TiO}_2(110)$ surface,⁵¹ whereas thermal catalytic studies of HCOOCH_3 formation from CH_3OH on $\text{Au}(111)$ ^{35–39} and $\text{PdO}(101)$ thin films⁵² all concluded that the cross-coupling reaction of CH_3O and CH_2O could occur below room temperature as a result of the easy attack of CH_2O by CH_3O . The earlier studies⁵¹ also indicated that the barrier for CH_2O dimerization is higher than that for the cross-coupling reaction of CH_3O and CH_2O . In our experiment, CH_3O might be more likely to react with adjacent CH_2O than to dissociate to produce additional CH_2O because the presence of bridge-bonded H atoms could inhibit the dissociation reaction, $\text{CH}_3\text{O} \rightarrow \text{CH}_2\text{O} + \text{H}$. An

increased likelihood for CH_3O to undergo a cross-coupling reaction than a dissociation reaction would prevent the build-up of CH_2O that would be available for self-coupling reactions. Indeed, Figure 3 suggests that the buildup of CH_2O is limited by the formation of HCOOCH_3 .

Friend and co-workers have proposed that the formyl radical (HCO) is an intermediate in the mechanism by which CH_3O and CH_2O react on a surface to produce HCOOCH_3 . HCO is presumably formed by the hole-mediated abstraction of an H atom by a BBO atom. The evidence for HCO comes from irradiating a surface of coadsorbed CH_2O and O. The observation of CO and CO_2 at high temperatures from a UV-irradiated $\text{TiO}_2(110)$ surface with coadsorbed CH_2O and O indicated the presence of formate and thus led to the conclusion that irradiation induces the loss of H, which would create an HCO intermediate. This conclusion is apparently at odds with an isotopic labeling study on the dehydrogenation of methanol to methyl formate over copper-based catalysts,⁵³ which ruled out an HCO intermediate in the coupling of methoxy and formaldehyde to form methyl formate. However, the different catalytic system might alter the mechanistic details. Nevertheless, the inference of an HCO intermediate based on formate formation is further called into question by recent investigations showing that a radical intermediate, RCO , is not required in the photoinduced transformation of acetone and acetaldehyde to formate on preoxidized $\text{TiO}_2(110)$.^{41–47} These studies have demonstrated that acetone or acetaldehyde adsorbed on preoxidized $\text{TiO}_2(110)$ undergoes a facile thermal reaction to form a photoactive acetone–oxygen or acetaldehyde–oxygen complex first, and then UV light irradiation of the acetone–oxygen or acetaldehyde–oxygen complex results in the ejection of a methyl radical into the gas phase and conversion of the surface bound fragment to acetate or formate.

We, too, observe evidence for formate when CH_2O is adsorbed on a $\text{TiO}_2(110)$ surface and irradiated (see Figure 10). The fact the formate is produced from CH_2O without coadsorbed oxygen suggests that one of the O atoms in the formate species comes from a BBO row. Formation of formate from CH_2O in the absence of coadsorbed oxygen does not necessarily imply an HCO intermediate, but such an intermediate might be possible. If HCO were formed, then formate production in conjunction with BBO atoms would be expected to compete with other reactions.

The use of isotopic substitution can be used to show that HCO (or DCO) is not an intermediate in the cross-coupling reaction that produces HCOOCH_3 (or DCOCD_3) under our experimental conditions. As seen in Figure S3, Supporting Information (and in our earlier study²⁴), when CD_3OH is used as the methanol precursor, CD_2O builds up on the surface but reacts only negligibly with CD_3O to produce DCOCD_3 . Thus, the final cross-coupling step is effectively blocked by the isotope effect, allowing the investigation of the state of CD_2O on a surface that is representative of the actual reactive system. Figure 11 shows various TPD spectra from such a surface that started with 0.5 ML of adsorbed CD_3OH , with three irradiation durations. After 60 min of irradiation, about 0.13 ML of CD_3OH is depleted (not including the small fraction of CD_3OH that undergoes an isotope exchange to form CD_3OD or reaction with oxygen vacancy sites), implying that 0.13 ML of CD_2O is formed (including adsorbed and photodesorbed CD_2O). Unlike the TPD spectra collected when CH_2O was adsorbed on the surface and irradiated (Figure 10), the $m/z = 28$ TPD spectrum from a CD_3OH -adsorbed and irradiated

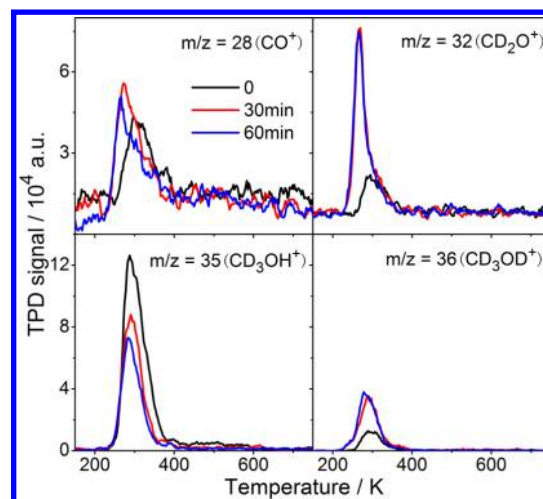


Figure 11. TPD spectra acquired at $m/z = 28(\text{CO}^+)$, $32(\text{CD}_2\text{O}^+)$, $35(\text{CD}_3\text{OH}^+)$, and $36(\text{CD}_3\text{OD}^+)$ from 0.5 ML of CD_3OH adsorbed on $\text{TiO}_2(110)$, with irradiation times of 0, 30, and 60 min, as shown.

surface exhibits no peak at 587 K (Figure 11), demonstrating that formate is not formed on this surface. The absence of formate indicates that DCO could not have been formed, which strongly suggests that HCO is not an intermediate in the cross-coupling reaction to produce HCOOCH_3 on $\text{TiO}_2(110)$. The reaction probably proceeds through a direct coupling of CH_3O and CH_2O , as has been proposed earlier as part of a hemiacetal mechanism.⁵³

The lack of apparent C–D bond dissociation from CD_2O on the CD_3OH -adsorbed surface vs C–H bond dissociation from CH_2O on the CH_2O -adsorbed surface might be explained by the availability of unoccupied BBO sites. When CD_3OH (or CH_3OH) undergoes stepwise photocatalytic dissociation, hydrogen atoms are transferred to BBO atoms. Thus, neighboring BBO sites would not be available to receive a hydrogen atom from CH_2O (or CD_2O), as they would be when only CH_2O is adsorbed on the surface. Even in a direct coupling mechanism, which does not involve an HCO intermediate, an H atom must be lost and inevitably go to a BBO site. Thus, at least one of the reactants, presumably CH_2O as a result of its relatively low adsorption energy, would be expected to require some mobility on the surface in order to react near a BBO site without an attached H atom. In an analogous TPD experiment conducted with irradiation at 355 nm, we have found that a modest increase in surface temperature dramatically enhances the production rate of HCOOCH_3 (Figure 12). The temperature-dependent production of HCOOCH_3 is consistent with the presumed requirement for surface mobility of CH_2O . Note that the surface temperature (180 K) at which HCOOCH_3 was observed to be formed is similar to the temperature (180 K) used in the experiment with CD_3OH from which we concluded that DCO (or HCO) cannot be an intermediate in the cross-coupling reaction. Thus, under conditions where there should be sufficient mobility to promote the cross-coupling reaction, we do not observe formate formation and can rule out the DCO (or HCO) intermediate. We therefore conclude that the mobility of CH_2O is not required to move it to a site where HCO can be formed; rather, we believe that it moves to a location where it can couple directly with CH_3O and lose its H atom to a BBO site. Instead of being mediated by hole formation on a BBO atom, as has been suggested,²³ the cross-

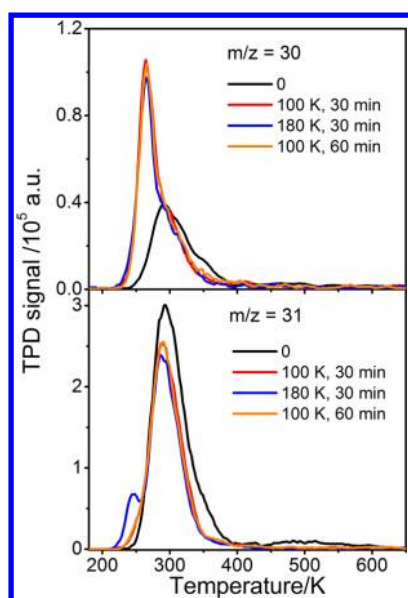


Figure 12. TPD spectra acquired at $m/z = 30(\text{CH}_2\text{O}^+)$ and $31(\text{CH}_3\text{O}^+)$, from 0.5 ML of CH_3OH adsorbed on $\text{TiO}_2(110)$, with irradiation at 355 nm. The laser flux was 1.27×10^{17} photons $\text{cm}^{-2} \text{s}^{-1}$ with a bandwidth of ~ 20 nm and a spot size of 6 mm. Irradiation times are noted in the figure. TPD spectra from the unirradiated surface and the low-temperature-irradiated surfaces followed initial adsorption at 100 K. With the low UV flux used, the surface temperature rose less than 5 K during irradiation of the low-temperature surfaces. The surface was maintained at a temperature of 180 K for the higher temperature irradiation. The TPD spectra indicate that CH_3OH can be photocatalyzed to CH_2O at 100 or 180 K but that CH_2O only reacts to produce HCOOCH_3 at the higher temperature.

coupling reaction might simply occur on the ground electronic state, promoted by localized surface heating from photon irradiation.

V. CONCLUSIONS

Our TPD results show strong evidence that the cross-coupling reaction, $\text{CH}_3\text{O} + \text{CH}_2\text{O} \rightarrow \text{HCOOCH}_3 + \text{H}$, is concurrent with the stepwise photocatalytic dissociation of CH_3OH on rutile $\text{TiO}_2(110)$ at an irradiation wavelength of 400 nm, where CH_3O and CH_2O are the products of the first and second steps and where initial coadsorption of oxygen is not necessary to initiate the process. This reaction takes place during irradiation, with longer irradiation times resulting in almost complete conversion of the CH_2O product into HCOOCH_3 . The reaction does not appear to involve an HCO intermediate and may proceed through direct coupling of CH_3O and CH_2O through a hemiacetal mechanism. The conclusion that HCO is not an intermediate suggests that a hole-mediated mechanism might not be operable in this reaction. The observation that HCOOCH_3 may be formed from a single precursor (CH_3OH) by irradiation at low temperatures further demonstrates the utility of TiO_2 as a photocatalyst for synthetic reactions, especially the esterification of alcohols. Further utility in photocatalytic reactions should come from a detailed understanding of the dynamical processes at the surface that channel photon energy into the reaction coordinate.

■ ASSOCIATED CONTENT

Supporting Information

Dependence of TPD signals on laser photon flux. TPD spectra at a variety of m/z ratios, verifying that methyl formate is formed rather than glycolaldehyde. Yields of CD_2O and DCOOCD_3 when a CD_3OH -adsorbed $\text{TiO}_2(110)$ surface is irradiated. Dependence of HCOOCH_3 TPD signal on initial coverage of CH_3OH . This material is available free of charge via the Internet at <http://pubs.acs.org>.

■ AUTHOR INFORMATION

Corresponding Author

*E-mail: tminton@montana.edu (T.K.M.); xmyang@dicp.ac.cn (X.Y.).

Author Contributions

[†]These authors have made similar contributions to this work.

Notes

The authors declare no competing financial interest.

[#]Chinese Academy of Sciences Visiting Senior Scientist.

■ ACKNOWLEDGMENTS

This work was supported by the Chinese Academy of Sciences, National Science Foundation of China, and the Chinese Ministry of Science and Technology. T.K.M. is grateful for support from the Chinese Academy of Sciences Visiting Professorships for Senior International Scientists.

■ REFERENCES

- (1) Al-Mazraoui, L. S.; Bowker, M.; Davies, P.; Dickinson, A.; Greaves, J.; James, D.; Millard, L. The Photocatalytic Reforming of Methanol. *Catal. Today* **2007**, *122*, 46–50.
- (2) Awate, S. V.; Deshpande, S. S.; Rakesh, K.; Dhanasekaran, P.; Gupta, N. M. Role of Micro-Structure and Interfacial Properties in the Higher Photocatalytic Activity of TiO_2 -Supported Nanogold for Methanol-Assisted Visible-Light-Induced Splitting of Water. *Phys. Chem. Chem. Phys.* **2011**, *13*, 11329–11339.
- (3) Chiarello, G. L.; Aguirre, M. H.; Selli, E. Hydrogen Production by Photocatalytic Steam Reforming of Methanol on Noble Metal-Modified TiO_2 . *J. Catal.* **2010**, *273*, 182–190.
- (4) Chiarello, G. L.; Ferri, D.; Selli, E. Effect of the $\text{CH}_3\text{OH}/\text{H}_2\text{O}$ Ratio on the Mechanism of the Gas-Phase Photocatalytic Reforming of Methanol on Noble Metal-Modified TiO_2 . *J. Catal.* **2011**, *280*, 168–177.
- (5) Mills, A.; Davies, R. H.; Worsley, D. Water Purification by Semiconductor Photocatalysis. *Chem. Soc. Rev.* **1993**, *22*, 417–425.
- (6) Diebold, U. The Surface Science of Titanium Dioxide. *Surf. Sci. Rep.* **2003**, *48*, 53–229.
- (7) Kominami, H.; Sugahara, H.; Hashimoto, K. Photocatalytic Selective Oxidation of Methanol to Methyl Formate in Gas Phase over Titanium(IV) Oxide in a Flow-Type Reactor. *Catal. Commun.* **2010**, *11*, 426–429.
- (8) Mancuso, A. J.; Huang, S. L.; Swern, D. Oxidation of Long-Chain and Related Alcohols to Carbonyls by Dimethyl-Sulfoxide Activated by Oxalyl Chloride. *J. Org. Chem.* **1978**, *43*, 2480–2482.
- (9) Henderson, M. A. A Surface Science Perspective on TiO_2 Photocatalysis. *Surf. Sci. Rep.* **2011**, *66*, 185–297.
- (10) Henderson, M. A.; Otero-Tapia, S.; Castro, M. E. The Chemistry of Methanol on the TiO_2 Surface: The Influence of Vacancies and Coadsorbed Species. *Faraday Discuss.* **1999**, *114*, 313–329.
- (11) Gamble, L.; Jung, L. S.; Campbell, C. T. Decomposition and Protonation of Surface Ethoxys on $\text{TiO}_2(110)$. *Surf. Sci.* **1996**, *348*, 1–16.

- (12) Brinkley, D.; Engel, T. Evidence for Structure Sensitivity in the Thermally Activated and Photocatalytic Dehydrogenation of 2-Propanol on TiO_2 . *J. Phys. Chem. B* **2000**, *104*, 9836–9841.
- (13) Farfan-Arribas, E.; Madix, R. J. Role of Defects in the Adsorption of Aliphatic Alcohols on the $\text{TiO}_2(110)$ Surface. *J. Phys. Chem. B* **2002**, *106*, 10680–10692.
- (14) Liu, Y. C.; Griffin, G. L.; Chan, S. S.; Wachs, I. E. Photo-Oxidation of Methanol Using: $\text{MoO}_3/\text{TiO}_2$ Catalyst Structure and Reaction Selectivity. *J. Catal.* **1985**, *94*, 108–119.
- (15) Cadson, T.; Griffin, G. L. Photooxidation of Methanol Using $\text{V}_2\text{O}_5/\text{TiO}_2$ and $\text{MoO}_3/\text{TiO}_2$ Surface Oxide Monolayer Catalysts. *J. Phys. Chem.* **1986**, *90*, 5896–5900.
- (16) Herman, G. S.; Dohnálek, Z.; Ruzyski, N.; Diebold, U. Experimental Investigation of the Interaction of Water and Methanol with Anatase- $\text{TiO}_2(101)$. *J. Phys. Chem. B* **2003**, *107*, 2788–2795.
- (17) Farfan-Arribas, E.; Madix, R. J. Different Binding Sites for Methanol Dehydrogenation and Deoxygenation on Stoichiometric and Defective $\text{TiO}_2(110)$ Surfaces. *Surf. Sci.* **2003**, *544*, 241–260.
- (18) Bates, S. P.; Gillan, M. J.; Kresse, G. Adsorption of Methanol on $\text{TiO}_2(110)$: A First-Principles Investigation. *J. Phys. Chem. B* **1998**, *102*, 2017–2026.
- (19) Sadeghi, M.; Liu, W.; Zhang, T.-G.; Stavropoulos, P.; Levy, B. Role of Photo-Induced Charge Carrier Separation Distance in Heterogeneous Photocatalysis: Oxidative Degradation of CH_3OH Vapor in Contact with Pt/TiO_2 and Cofumed $\text{TiO}_2\text{-Fe}_2\text{O}_3$. *J. Phys. Chem.* **1996**, *100*, 19466–19474.
- (20) Onda, K.; Li, B.; Zhao, J.; Petek, H. The Electronic Structure of Methanol Covered $\text{TiO}_2(110)$ Surfaces. *Surf. Sci.* **2005**, *593*, 32–37.
- (21) Yamakata, A.; Ishibashi, T.-A.; Onishi, H. Electron- and Hole-Capture Reactions on Pt/TiO_2 Photocatalyst Exposed to Methanol Vapor Studied with Time-Resolved Infrared Absorption Spectroscopy. *J. Phys. Chem. B* **2002**, *106*, 9122–9125.
- (22) Yurdakal, S.; Palmisano, G.; Loddo, V.; Augugliaro, V.; Palmisano, L. Nanostructured Rutile TiO_2 for Selective Photocatalytic Oxidation of Aromatic Alcohols to Aldehydes in Water. *J. Am. Chem. Soc.* **2008**, *130*, 1568–1569.
- (23) Phillips, K. R.; Jensen, S. C.; Baron, M.; Li, S. C.; Friend, C. M. Sequential Photo-Oxidation of Methanol to Methyl Formate on $\text{TiO}_2(110)$. *J. Am. Chem. Soc.* **2013**, *135*, 574–577.
- (24) Guo, Q.; Xu, C.; Ren, Z.; Yang, W.; Ma, Z.; Dai, D.; Fan, H.; Minton, T. K.; Yang, X. Stepwise Photocatalytic Dissociation of Methanol and Water on $\text{TiO}_2(110)$. *J. Am. Chem. Soc.* **2012**, *134*, 13366–13373.
- (25) Zehr, R. T.; Henderson, M. A. Influence of O_2 -Induced Surface Roughening on the Chemistry of Water on $\text{TiO}_2(110)$. *Surf. Sci.* **2008**, *602*, 1507–1516.
- (26) Henderson, M. A.; Shen, M. Identification of the Active Species in Photochemical Hole Scavenging Reactions of Methanol on TiO_2 . *J. Phys. Chem. Lett.* **2011**, *2*, 2707–2710.
- (27) Lu, G.; Linsebigler, A.; Yates, J. T., Jr. Ti^{3+} Defect Sites on $\text{TiO}_2(110)$: Production and Chemical Detection of Active Sites. *J. Phys. Chem.* **1994**, *98*, 11733–11738.
- (28) Schwaner, A. L.; White, J. M. Electron-Induced Chemistry of Methanol on $\text{Ag}(111)$. *J. Phys. Chem. B* **1997**, *101*, 10414–10422.
- (29) Hydroxy-Acetaldehyde, <http://webbook.nist.gov/cgi/cbook.cgi?ID=C141468&Units=SI&Mask=200>. Methyl Formate, <http://webbook.nist.gov/cgi/cbook.cgi?ID=C107313&Units=SI&Mask=200>.
- (30) Li, Z.; Smith, R. S.; Kay, B. D.; Dohnálek, Z. Determination of Absolute Coverages for Small Aliphatic Alcohols on $\text{TiO}_2(110)$. *J. Phys. Chem. C* **2011**, *115*, 22534–22539.
- (31) Tonner, S. P.; Trimm, D. L.; Wainwright, M. S.; Cant, N. W. Dehydrogenation of Methanol to Methyl Formate Catalysts. *Ind. Eng. Chem. Prod. Res. Dev.* **1984**, *23*, 384–388.
- (32) Domokos, L.; Katona, T.; Molmir, A. Dehydrogenation of Methanol to Methyl Formate: Deuterium Labeling Studies. *Catal. Lett.* **1996**, *40*, 215–221.
- (33) Minyukova, T. P.; Simentsova, I. I.; Khasin, A. V.; Shtertser, N. V.; Baronskaya, N. A.; Khassin, A. A.; Yurieva, T. M. Dehydrogenation of Methanol over Copper-Containing Catalysts. *Appl. Catal., A* **2002**, *237*, 171–180.
- (34) Liu, J.; Zhan, E.; Cai, W.; Li, J.; Shen, W. Methanol Selective Oxidation to Methyl Formate over $\text{ReO}_x/\text{CeO}_2$ Catalysts. *Catal. Lett.* **2008**, *120*, 274–280.
- (35) Abad, A.; Concepcion, P.; Corma, A.; Garcia, H. A Collaborative Effect between Gold and a Support Induces the Selective Oxidation of Alcohols. *Angew. Chem., Int. Ed.* **2005**, *44*, 4066–4069.
- (36) Nielsen, I. S.; Taarning, E.; Egeblad, K.; Madsen, R.; Christensen, C. H. Direct Aerobic Oxidation of Primary Alcohols to Methyl Esters Catalyzed by a Heterogeneous Gold Catalyst. *Catal. Lett.* **2007**, *116*, 35–40.
- (37) Xu, B.; Liu, X.; Haubrich, J.; Madix, R. J.; Friend, C. M. Selectivity Control in Gold-Mediated Esterification of Methanol. *Angew. Chem., Int. Ed.* **2009**, *48*, 4206–4209.
- (38) Xu, B.; Haubrich, J.; Freyschlag, C. G.; Madix, R. J.; Friend, C. M. Oxygen-Assisted Cross-Coupling of Methanol with Alkyl Alcohols on Metallic Gold. *Chem. Sci.* **2010**, *1*, 310–314.
- (39) Xu, B.; Liu, X.; Haubrich, J.; Friend, C. M. Vapour-Phase Gold-Surface-Mediated Coupling of Aldehydes with Methanol. *Nat. Chem.* **2010**, *2*, 61–65.
- (40) Henderson, M. A. Complexity in the Decomposition of Formic Acid on the $\text{TiO}_2(110)$ Surface. *J. Phys. Chem. B* **1997**, *101*, 221–229.
- (41) Henderson, M. A. Acetone Chemistry on Oxidized and Reduced $\text{TiO}_2(110)$. *J. Phys. Chem. B* **2004**, *108*, 18932–18941.
- (42) Henderson, M. A. Photooxidation of Acetone on $\text{TiO}_2(110)$: Conversion to Acetate via Methyl Radical Ejection. *J. Phys. Chem. B* **2005**, *109*, 12062–12070.
- (43) Henderson, M. A. Relationship of O_2 Photodesorption in Photooxidation of Acetone on TiO_2 . *J. Phys. Chem. C* **2008**, *112*, 11433–11440.
- (44) Henderson, M. A. Effect of Coadsorbed Water on the Photodecomposition of Acetone on $\text{TiO}_2(110)$. *J. Catal.* **2008**, *256*, 287–292.
- (45) Yasuo, M.; Sasahara, A.; Onishi, H. Acetone Adsorption on Oxidized and Reduced $\text{TiO}_2(110)$: A Scanning Tunneling Microscope Study. *J. Phys. Chem. C* **2010**, *114*, 14579–14582.
- (46) Zehr, R. T.; Henderson, M. A. Thermal Chemistry and Photochemistry of Hexafluoroacetone on Rutile $\text{TiO}_2(110)$. *Phys. Chem. Chem. Phys.* **2010**, *12*, 8084–8091.
- (47) Wilson, D. P.; Sporleder, D.; White, M. G. Final State Distributions of Methyl Photoproducts from the Photooxidation of Acetone on $\text{TiO}_2(110)$. *J. Phys. Chem. C* **2012**, *116*, 16541–16552.
- (48) Sánchez de Armas, R.; Oviedo, J.; San Miguel, M. A.; Sanz, J. F. Methanol Adsorption and Dissociation on $\text{TiO}_2(110)$ from First Principles Calculations. *J. Phys. Chem. C* **2007**, *111*, 10023–10028.
- (49) Oviedo, J.; Sánchez de Armas, R.; San Miguel, M. A.; Sanz, J. F. Methanol and Water Dissociation on $\text{TiO}_2(110)$: The Role of Surface Oxygen. *J. Phys. Chem. C* **2008**, *112*, 17737–17740.
- (50) Zhao, J.; Yang, J.; Petek, H. Theoretical Study of the Molecular and Electronic Structure of Methanol on a $\text{TiO}_2(110)$ Surface. *Phys. Rev. B* **2009**, *80*, 235416.
- (51) Kim, J.; Kay, B. D.; Dohnálek, Z. Formaldehyde Polymerization on $(\text{WO}_3)_3/\text{TiO}_2(110)$ Model Catalyst. *J. Phys. Chem. C* **2010**, *114*, 17017–17022.
- (52) Hakanoglu, C.; Hinojosa, J. A., Jr.; Weaver, J. F. Oxidation of Methanol on a $\text{PdO}(101)$ Thin Film. *J. Phys. Chem. C* **2011**, *115*, 11575–11585.
- (53) Cant, N. W.; Tounner, S. P.; Trimm, D. L.; Wainwright, M. S. Isotopic Labeling Studies of the Mechanism of Dehydrogenation of Methanol to Methyl Formate over Copper-Based Catalysts. *J. Catal.* **1985**, *91*, 197–207.